molecules

MDPI

Article

Synthesis of Fluorogenic Arylureas and Amides, and Their Interaction with Amines: A Competition Between Turn-on Fluorescence and Organic Radicals on the Way to a Smart Label for Fish Freshness.

Javier García-Tojal, José V. Cuevas, M. Josefa Rojo, Borja Díaz de Greñu, Carla Hernando-Muñoz, José García-Calvo, Mateo M. Salgado, Tomás Torroba *

Department of Chemistry, Faculty of Science, University of Burgos, 09001 Burgos, Spain; qipgatoj@ubu.es
* Correspondence: ttorroba@ubu.es

Abstract: We describe the synthesis of fluorogenic arylureas and amides, and their interaction with primary or secondary amines under air and light in organic-aqueous mixtures to give rise to a new class of persistent organic radicals, described on the basis of their EPR, UV-Vis, fluorescence, NMR, and quantum mechanics calculations, and their prospective use as multi-signal reporters in a smart label for fish freshness.

Keywords: Arylureas; Turn-on fluorescence; Organic radicals; Smart label; Volatile amines

Citation: García-Tojal, J.; Cuevas, J. V.; Rojo, M. J.; Díaz de Greñu, B.; Hernando-Muñoz, C.; García-Calvo, J.; Torroba, T. Synthesis of Fluorogenic Arylureas and Amides, and Their Interaction with Amines: A Competition Between Turn-on Fluorescence and Organic Radicals on the Way to a Smart Label for Fish Freshness. *Molecules* **2021**, *26*, x. https://doi.org/10.3390/xxxxx

Academic Editor: Firstname Lastname
Received: date
Accepted: date
Published: date

1. Introduction

Persistent organic radicals are of immense importance for the preparation of new hybrid materials in spin-probe and spin-label functions,[1] magnetic materials,[2] electrical transport,[3] molecular spintronics[4] and surface-confined electroactive molecules for single molecule switching devices,[5] and are still important in classical areas such as catalysis for the oxidation of organic molecules,[6] and DNA damage.[7] Persistent radical cations[8] and radical anions,[9] examples of organic mixed-valence compounds,[10] are also important, such as their neutral organic radicals parents, for the discovery of new organic materials and the development of improved devices. Amines and their derivatives are extensively used chemicals as abuse drugs, cosmetics, polymers, etc.[11] They are also important markers for food industries and medical diagnosis, being involved in many biological processes as neurotransmitters.[12] The detection and discrimination of amines is an important issue in environmental protection and human health. Common protocols for amine analyses are based on chromatographic methods,[13] which are quite time-consuming; therefore the development of fluorescent sensors for amines has become a desirable alternative given their simple instrumentation and fast response time, albeit a lack of selectivity in some examples,[14-18] but the use of multiple signaling sensors can remediate this adverse selectivity. Herein, we present an unusual family of new fluorogenic aminoaryl-indane-based probes which are also able to form persistent radical species in the presence of primary or secondary amines and their prospective use as multiple signal fluorogenic reporters for the detection of volatile amines.

2. Results and Discussion

The synthesis of arylureas used along the paper was performed by an easy Suzuki reaction between 5-bromoindanone and 4-aminobenzeneboronic acid pinacol ester, followed by Knoevenagel reaction with malononitrile and reaction with selected mono and

bis-isocyanates (Scheme 1). For comparison of their fluorogenic properties, selected bis-amides were also prepared by straightforward reaction of the starting aminoindane derivative and acid chlorides (Scheme 1).

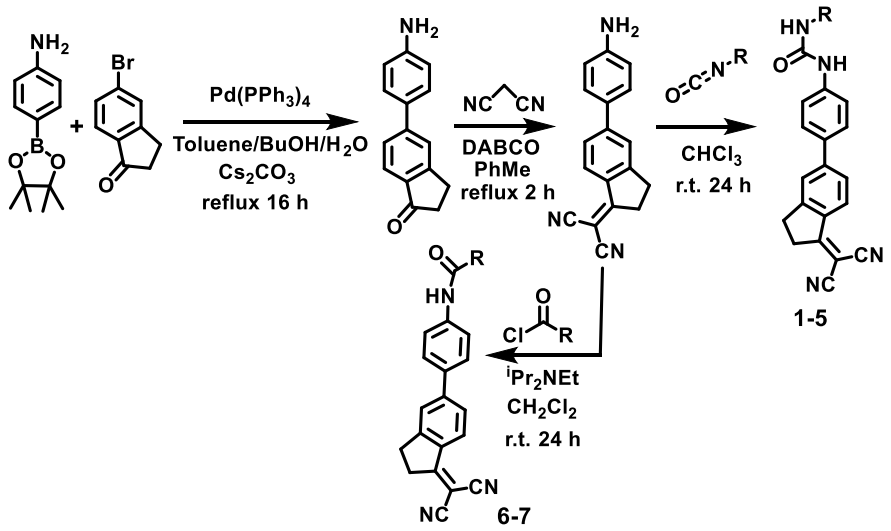

Scheme 1. Synthesis of the chemical probes.

In this way, chemical probes **1**-**7** were prepared (Figure 1). Probe **1** was previously reported as an excellent fluorogenic sensor for the determination of 3,4-methylenedioxymethamphetamine (MDMA) from ecstasy tablets.[19] The interaction of primary and secondary amines and the fluorogenic probe was the key step in their selective discrimination from tertiary amines, anilines or heterocyclic amines. We observed that the presence of primary or secondary biogenic amines initially promoted a sudden fluorescence in the probe, which was followed by gradual emission extinction.

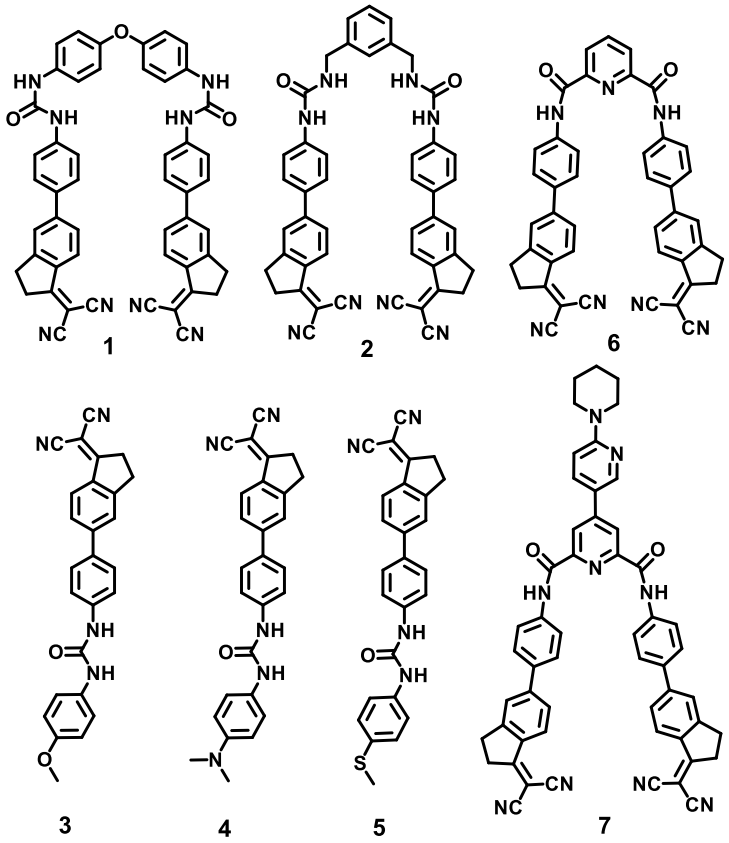

Figure 1. Chemical structures of the studied chemical probes.

The kinetics of the process was specific for every reported amine, but the reason for the emission extinction was unclear until we noticed that it was caused by the presence of radical species generated after the probe/amine interaction. We selected a typical amine derivative, pyrrolidine, and studied the interaction of pyrrolidine and **1** by titration experiments in EPR, NMR, UV-vis and fluorescence spectroscopy in order to understand the type of interaction involved in the generation of radical species. First, the effect of the addition of pyrrolidine to an equimolecular solution of the bis-diarylurea **1** in dimethylsulfoxide (DMSO) was studied by X-band EPR measurements at room temperature under room light and air. A time-dependent absorption was obtained after a faint discoloration of the dark orange solution of **1**. The signal was sensitive to the solvents used. Though the low solubility of **1** compelled to use DMSO, the only common solvent in which this urea was moderately soluble, a continuous decrease in the intensity of the EPR signal since minute 5 was observed if DMSO was used as the unique solvent. However, the radical life-time increased with the addition of water, therefore aqueous mixtures were used for the measurements. In some of the experiments acetone was added in an attempt to improve the resolution by diminishing the viscosity of the solvent mixture, albeit no highly significant improvement was attained. As a typical example, Figure 2 shows the evolution with time of the EPR spectra for a mixture of **1** and pyrrolidine at room temperature. The measurements were performed on a mixture prepared from 100 μl of 10^{-2} M stock solution of **1** in DMSO diluted with 100 μl of water, 100 μl of acetone and 100 μl of DMSO, stirred for 1 h and then followed by addition of 100 μl of a 10^{-2} M solution of pyrrolidine in DMSO. After shaking, 200 μl of the non-deoxygenated mixture were pipetted into a flat cell. A spectrum with eighteen equally spaced lines was registered at room temperature, whose intensity increased for the first 11−12 minutes and then decreased to disappearance within the next 40 h. (Figure 2)

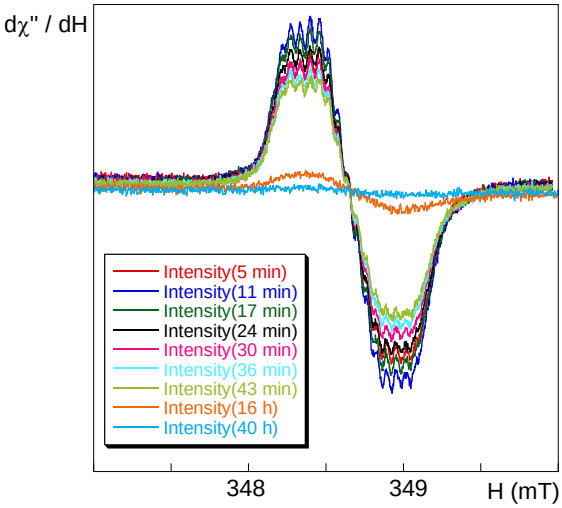

Figure 2. EPR spectral evolution with time for an equimolecular solution of **1** and pyrrolidine. Experimental details of the data collection: modulation amplitude 0.1 mT, time constant 40.96 ms, conversion time 327.68 ms, gain 6.32×10^4, power 20 mW and microwave frequency 9.7410 (5 min), 9.7410 (11 min), 9.7410 (17 min), 9.7410 (24 min), 9.7460 (30 min), 9.7410 (36 min), 9.7410 (43 min), 9.7410 (16 h), and 9.7760 (40 h) GHz.

Once the experimental conditions were optimized, the best protocol consisted in preparing an orange mixture containing 100 µl of 10^{-2} M stock solution of **1** in DMSO, diluted by addition of 100 µl of water and 200 µl of DMSO, stirred for 2 hours and then followed by addition of 100 µl of a 10^{-2} M solution of pyrrolidine in DMSO, in which moment the color of the mixture faintly clarified. After shaking, 200 µl of the final solution (2×10^{-3} M in DMSO/water 4:1 v/v) were pipetted into a flat cell where the measurements started 11 min after the addition of the amine. The obtained spectrum is shown in Figure 3. The best fit (correlation coefficient R = 0.9930) was reached taking into account the hyperfine coupling of the unpaired electron to two non-equivalent ^{14}N nitrogen nuclei (I = 1) and three sets of non-equivalent ^{1}H hydrogen atoms (I = ½). The parameters arisen from the fit were: g = 2.0035, A_{N1} = 0.180 mT (1N, 1.68 10^{-4} cm^{-1}), A_{N2} = 0.060 mT (1N, 0.56×10^{-4} cm^{-1}), A_{H1} = 0.260 mT (1H, 2.43×10^{-4} cm^{-1}), A_{H2} = 0.120 mT (2H, 1.12×10^{-4} cm^{-1}), A_{H3} = 0.060 mT (2H, 0.56×10^{-4} cm^{-1}), line-width ΔH = 0.055 mT.

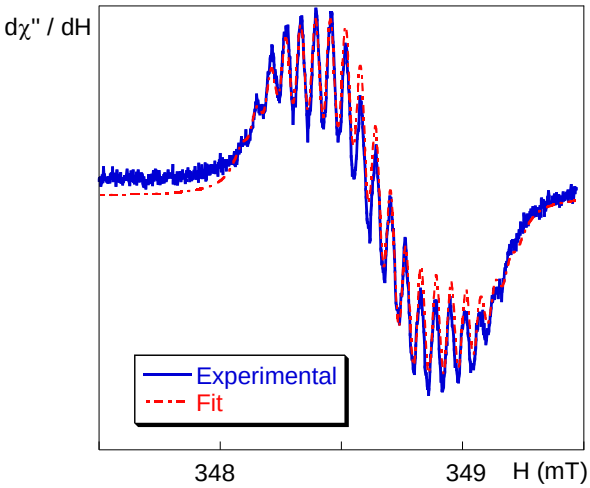

Figure 3. Experimental (blue line) and simulated (dashed red line) EPR spectra of radical **[1]**• in DMSO/water. Experimental details: modulation amplitude 0.02 mT, time constant 40.96 ms, conversion time 327.68 ms, gain 6.32×10^4, power 20 mW and microwave frequency 9.7768 GHz.

The use of *n*-butylamine instead of pyrrolidine yielded a similar spectrum. A comparison between the EPR spectra of **1** after addition of pyrrolidine or *n*-butylamine is given in Figure 4; the experimental conditions are the same given for previous pyrrolidine experiments, the microwave frequency in the case of the *n*-butylamine was 9.7750 GHz. An equimolecular solution of **1** and DABCO in similar conditions gave rise to a very weak isotropic signal with non-resolved hyperfine structure (g ≈ 2.0035, ΔH = 0.500 mT (Figure S29 in the Supporting Information [SI]). In the case of the interaction of **1** with tetrabutylammonium cyanide, signals weaker than those obtained from **1** and pyrrolidine were registered, but they showed the same hyperfine pattern (Figure S30, SI). On the contrary, a very weak and unresolved initial signal was obtained when aqueous NaOH 1 M solution was added (SI). After one day, this signal evolved to an intense isotropic gaussian-type signal (g = 2.0029, ΔH = 0.580 mT) while the color of the solution turned into dark green (Figure S31, SI).

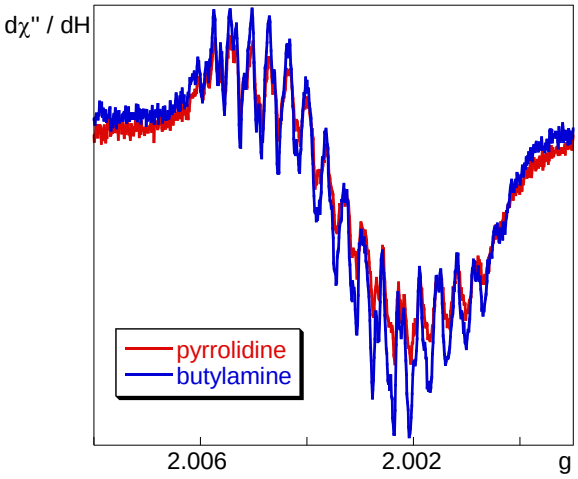

Figure 4. EPR spectra for the interaction of an equimolecular solution (2 × 10^{-3} M in DMSO/water 4:1 v/v) of **1** and pyrrolidine or *n*-butylamine. The measurements started at 20 min (pyrrolidine) and 6 min (*n*-butylamine) after the addition of the amine. Experimental details of the data collection: modulation amplitude 0.01 mT, time constant 40.96 ms, conversion time 327.68 ms, gain 6.32 × 10^4, power 20 mW in all cases. Microwave frequency 9.7718 (pyrrolidine, 3 scans) and 9.7713 GHz (*n*-butylamine, 4 scans).

The EPR results proceeded in parallel to the reported fluorescent results for **1** which was only sensitive to the presence of primary and secondary amines, generating an intense fluorescent signal, but it was not sensitive to the presence of tertiary amines, with the exception of a weak sensitivity to DABCO.[19] We then recorded the EPR spectra of the bis(aryl-benzyl)urea **2** (a fluorescent molecular ruler for ω-aminoacids),[20] the bisarylureas **3-5** and the diamides **6** and **7** (the central diamide linker was used in fluorescent polyamide chemical probes)[21] in the presence of 1 equiv. of pyrrolidine in the same conditions. In spite of their low intensities and deficient resolutions, the measurements performed on those bis- and monoureas suggested the attainment of the same EPR signal with different intensities, being the most intense signals those related with the bisurea systems in the order: **1** >> **2** > **3** ≈ **4** ≈ **5** indicating that the bis-aryl-urea **1** produced a more intense and better resolved signal than bis-benzylurea **2** and both produced more intense signals than mono-arylureas **3-5**. However, no signal in EPR spectra were obtained in the experiments with the bis-amides **6-7** under the same experimental conditions, therefore there were no further studied (Figure 5).

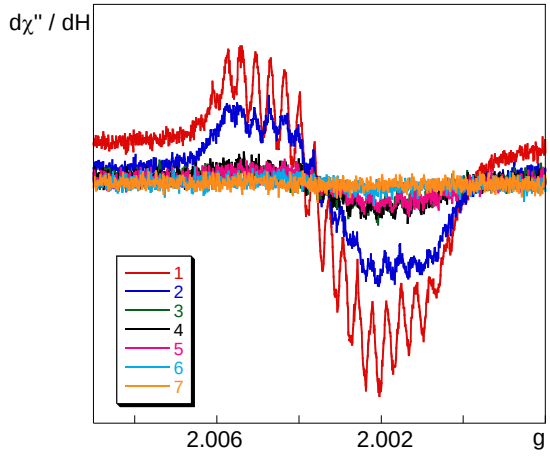

Figure 5. A comparison of the EPR spectra of **1**–**7** with pyrrolidine, 2 × 10^{-3} M equimolecular solutions in DMSO/water 4:1 v/v. The measurements were carried out 11 min after the addition of the amine. Experimental details of the data collection: modulation amplitude 0.02 mT, time constant 40.96 ms, conversion time 327.68 ms, gain 6.32 × 10^4, power 20 mW and three scans in all cases. Microwave frequencies 9.7732 (**1**), 9.7726 (**2**), 9.7724 (**3**), 9.7727 (**4**), 9.7716 (**5**), 9.7713 (**6**) and 9.7715 GHz (**7**).

EPR intensity changes were accompanied by changes in the color of the solution, from orange to pale yellow, after the addition of the amine to **1-5** solutions, therefore we performed UV-vis and fluorescence titrations with **1** and pyrrolidine, as a representative case, under the same conditions, generating changes in color and an intense fluorescent signal either in mixed solvents, DMSO/water/acetone, or pure DMSO, that was also followed by kinetic measurements (see Figures S36 to S41 in the Supporting Information). Addition of up to some equivalents of pyrrolidine in DMSO to a solution of **1**, 5.0 × 10^{-5} M, in DMSO at room temperature caused the appearance of a UV-Vis absorption band centered at 305 nm and the disappearance of the absorption band centered at 405 nm (SI). In the interval between 0 and 1 equiv. of amine an isosbestic point at 336 nm was observed. Along the titration experiment we did not observe bands in the 650-900 nm region of the absorption spectrum, which are characteristics of the formation of radical anion species,[22-23] so their presence was discarded. UV-Vis titration experiments in a DMSO/water 4:1 (v/v) mixture gave similar results. We calculated the binding constants from UV-vis and fluorescence titrations (SI), which were in agreement with those previously reported for biogenic amines.[19] Therefore the behavior of **1** in the presence of pyrrolidine was similar to the observed for related amines so we assumed that the radical species was formed in the presence of all reported primary or secondary amines.

The evolution of the radical species was followed by ^{1}H and ^{13}C NMR spectroscopy of equimolecular solutions 2.5 × 10^{-3} M of **1** and pyrrolidine in deuterated DMSO. The ^{1}H NMR spectrum of **1** is shown in Figure 6, in blue. Recording of the spectrum immediately after addition of pyrrolidine gave the purple spectrum in Figure 6, that showed upfield displacements in one of the NH peaks near δ 9.0, the closest aromatic proton signal at δ 8.25 (the aromatic proton signals between δ 7.5-8.0 also experienced upfield changes) and downfield displacement of one of the methylene groups at δ 3.2, indicated by the blue and purple arrows, but the resolution of the spectrum did not experience changes, indicating only hydrogen bond interactions. Recording of the spectrum of the same sample after 8 hours gave the green spectrum in Figure 6, in which the NH protons gave a broad signal near 9 ppm, all aromatic protons between δ 7.3 and δ 8.3 gave a large unresolved signal between δ 8-7.6 and the methylene signals appeared as large multiplets between δ 3-3.5, indicating a strong perturbation of the resolution (green arrows). The signals at δ 7.5 and δ 7 did not experience large changes.

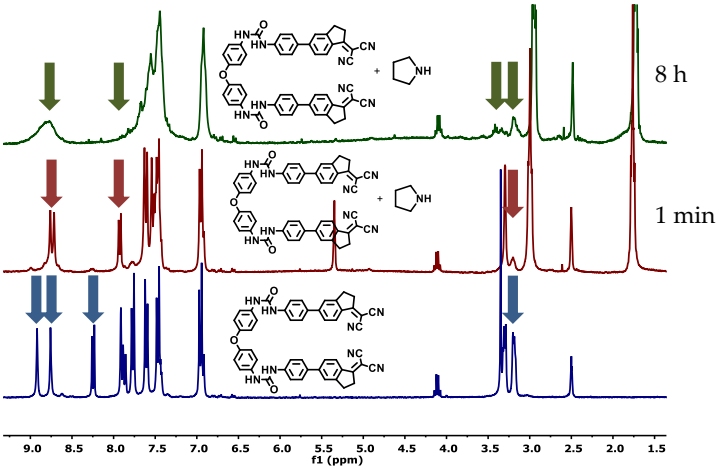

Figure 6. Evolution of the ^{1}H NMR spectrum of equimolecular solutions 2.5 × 10^{-3} M of **1** + pyrrolidine in DMSO-*d*$_6$.

The ^{13}C NMR spectrum of **1** is shown in Figure 7, in blue. Recording of the spectrum for 8 hours after addition of pyrrolidine gave the purple spectrum in Figure 7, that showed disappearance of the signals at δ 180 and δ 70 (corresponding to the exocyclic double bond), of the two peaks at around δ 114 (corresponding to the two cyano groups) and the methylene signal near δ 30. These changes are indicated by the blue and purple arrows. The spectrum showed also appearance of a new cyano group signal at δ 109, indicated by the red arrow. The signal by δ 155 diminished and the rest of aromatic carbon signals between δ 150 and δ 123 experienced several changes, but the signals between δ 120-118 remained unchanged. Apparently, the bis-aryl ether moiety was not affected by the presence of the radical species, neither in ^{1}H NMR nor in ^{13}C NMR spectra, but all changes were experienced in the arylindane moiety. The most important changes affected to the exocyclic dicyanovinyl group and the closest methylene group, indicating the main positions where the radical species was localized. The signals corresponding to the pyrrolidine group remained unchanged in all spectra.

We hypothesized that addition of an electron to the cyanovinyl moiety produced a weakening of the triple bond that thus accumulated negative charge on the nitrogen acquiring a more C=N character, a structure that can be stabilized by hydrogen capture, or C=C=N··H group, in the presence of water. Both IR and NMR data pointed to the weakening of the C≡N bond in agreement with this hypothesis.

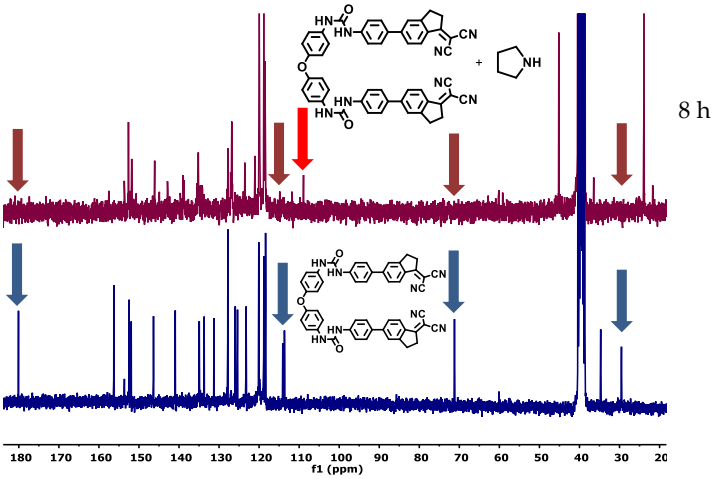

Figure 7. Evolution of the ^{13}C NMR spectrum of equimolecular solutions 2.5 × 10^{-3} M of **1** + pyrrolidine in DMSO-*d*$_6$.

A structure featuring all facts was subjected to quantum chemical calculations, as shown in Figure 8. Geometric structure of [**1**]• was optimized by using the Becke three-parameter functional[24] and the Lee–Yang–Parr correlation functional[25] (B3LYP) at the 6-31G* basis set for all the elements such as implemented in the Gaussian 03 (Revision C.02) program suite.[26] The unrestricted protocol was used for open-shell systems. From the energy optimized structures, the singly occupied molecular orbital, SOMO is represented in Figure 7. The SOMO is centered on the dicyanovinyl moiety and displays a π-antibonding character located over the C=N bond of the protonated nitrogen and over the 1-indan carbon atom and the aryl group, as well as π-bonding over the indane aryl group. The molecular orbital has slight contributions of σ-bonding interactions between the hydrogen atom and the ketenimine nitrogen atom as well as the hydrogen atoms from the alpha-methylene carbon atom of the five membered ring. The large electronic delocalization seems to be responsible for the high stability and long life of the radical. The SOMO+1 was located on the arm of the molecule not affected by the formation of the radical. It has mainly π-antibonding character located over the aryl fragment near to the nitrile groups, and π-antibonding character in the nitrile groups. Nevertheless, this orbital has slight π-bonding character in the C-C interactions of the nitrile groups and the 1-indane carbon atom with the aryl fragment. The SOMO+1 was 2.03 eV (195.65 kJ mol^{-1}, 46.76 kcal mol^{-1}) higher in energy than SOMO. The SOMO-1 is a π-bonding molecular orbital delocalized over the phenyl rings directly bonded to the ether oxygen atom and with slight π-antibonding interactions with a p orbital of this oxygen atom and with p orbitals of the urea nitrogen atoms. The SOMO-1 was 1.03 eV (99.24 kJ mol^{-1}, 23.72 kcal mol^{-1}) lower in energy than SOMO. The energy gap between SOMO and SOMO+1 was within the visible light region, 1.55-3.26 eV (150-315 kJ mol^{-1}, 35.85-75.29 kcal mol^{-1}) therefore light excitation and proton transfer may delocalize the radical between both arylindane moieties. This fact explains the fact that in $^{1}H/^{13}C$ NMR both arylindane groups seem to be affected in the same extension by the formation of the radical species. The interaction must be intramolecular. Indeed, a mixture of **1**, pyrrolidine and 5-(4-aminophenyl)-1-dicyanomethylene-indane (the amine precursor of **1**) in deuterated DMSO, showed the vinyl signals at δ 180 and δ 70 after 8 hours ^{13}C NMR recording. The fact that the SOMO-1 was localized exclusively at the diarylether moiety explained the fact that this group appeared unchanged in all spectroscopic experiments. Although the diarylether group seems to have little influence in the stability of the radical species (there is no electronic interaction) this link seems to be optimal for electron delocalization between both indane moieties. An electronically isolated link such as the *m*-xylyl group in **2** produced a much weaker radical species in similar conditions and all conjugated bis-amide links such as in **6-7** did not produce radical species in the presence of pyrrolidines.

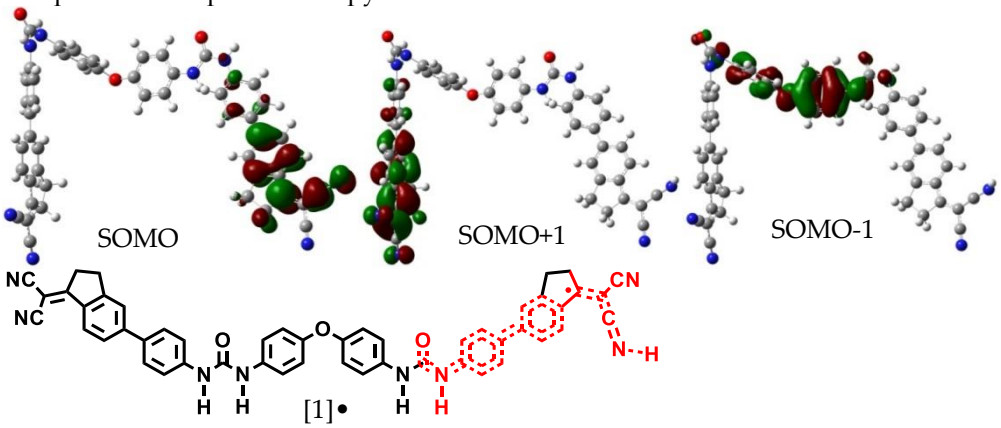

Figure 8. SOMO, SOMO+1 and SOMO-1 for compound [**1**]•.

From previous background and the new experiments, we assumed that compound **1** was a non-fluorescent compound, in contrast to the fluorescent compound **2**, because of

charge transfer from the diarylether moiety to the fluorescent arylindane groups. Addition of primary or secondary amines such as pyrrolidine or *n*-butylamine inhibited the charge transfer by forming hydrogen bonds, thus giving rise to a fluorescent intermediate that underwent electron transfer[27] from the amine group to the indane moiety, facilitated by simultaneous proton transfer from water,[28] giving rise to radical species characterized by several spectroscopic techniques (Figure 9). A quick inspection to the evolution of fluorescence (left) and paramagnetic signal (EPR, right) in Figure 9 clearly showed that extinction of fluorescence evolved in parallel to the increase of the EPR signal so that reaching the asymptotic minimum in fluorescence happened at roughly the same time that the maximum in EPR signal was reached. We only observed the stable radical species [**1**]•, therefore the radical species that could form from the amine were reversed in the presence of water and air to the neutral amine, that appeared unchanged in all NMR experiments.

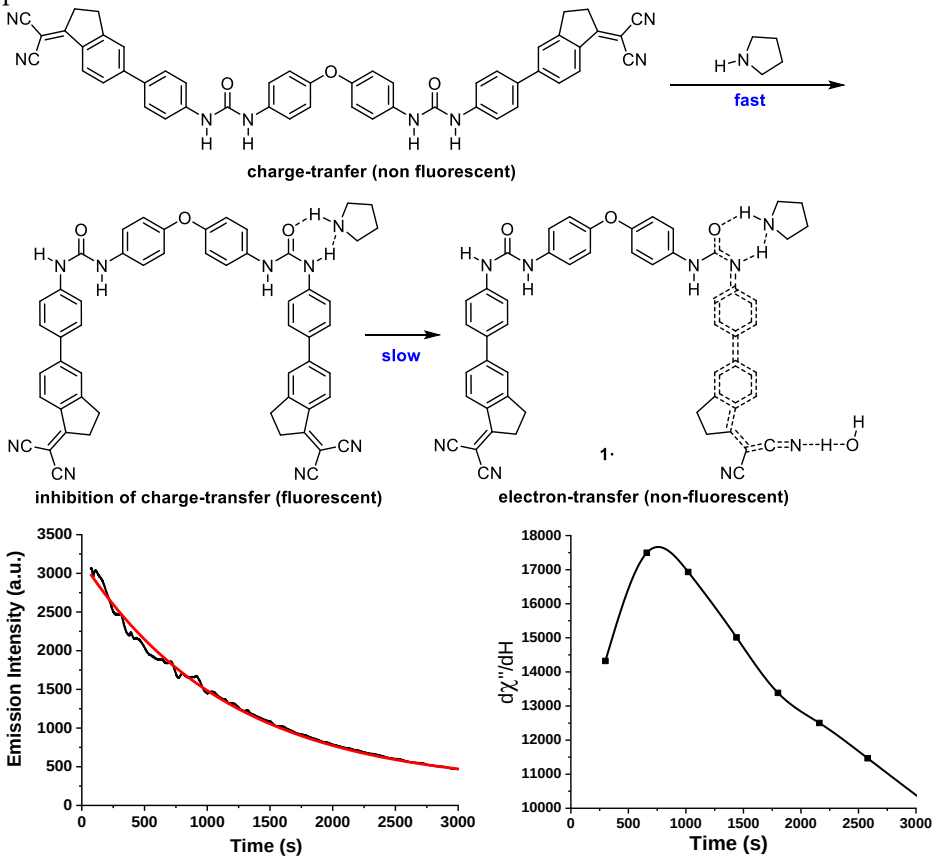

Figure 9. (Up) A summary of the formation and evolution of [**1**]•. (Bottom left) Fluorescence measured (black line) and fitting curve (red line) for the fluorescence intensity decay process of a 10:1 pyrrolidine/**1** solution, concentration C_1= 5.0 × 10−5 M in 3:1:1 (v/v) DMSO/water/acetone. (Bottom right) EPR spectral evolution with time for a solution of **1** and pyrrolidine in DMSO/water/acetone, under the conditions reported in Figure 2.

These chemical probes are the first examples of multi-signal reporters for the discrimination between primary, secondary and tertiary amines in which the usual signaling report by UV-visible or fluorescent signal is complemented by paramagnetic signaling of the same samples at different reporting times. The selectivity of the chemical probes for different types of amines and the large types of signaling offered by these probes, from now including paramagnetic species, will make them good starting points for the preparation of multi-signaling chemical probes for the detection of biogenic amines such as histamine, putrescine and cadaverine. These amines were of particular interest due to their characteristics as a marker for freshness in fish samples. To compare the different increase in fluorescence, the quantum yield of **1** was measured in DMSO in the presence of

pyrrolidine, used as a reference, and then histamine, putrescine or cadaverine, just after addition of amine. The reference was quinine sulfate in H_2SO_4 0.05M (Figure 10). The results were very similar for all of them, being a bit higher for pyrrolidine than for the rest of amines within the error of the method (±0.02). In all cases there was a quite noticeable fluorescent increase.

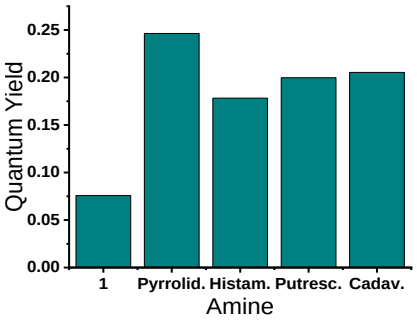

Figure 10. Quantum Yield of different combinations between **1** and amines in DMSO, comparation between: **1** without amine, pyrrolidine, histamine, putrescine, and cadaverine.

After testing in different conditions, the best conditions for the experiments were: three mackerel (*scomber scombrus*) samples were bought in a local market, the fish was cleaned, the spines were retired, and the muscle was grinded (Philips HR 28308/B). Then, samples of 10±0.2 g of fish were distributed in 20 ml vials and sealed with a septum. Half of the samples were incubated at 4 °C and half at 25±1 °C. Then, 3 ml of the gas phase of the vial were taken with a syringe and bubbled into a probe solution at different times as the fish decayed on time. The samples were measured in absorbance and fluorescence at their maximum peaks, the differences between the obtained values and a reference solution were plotted (Figure 11).

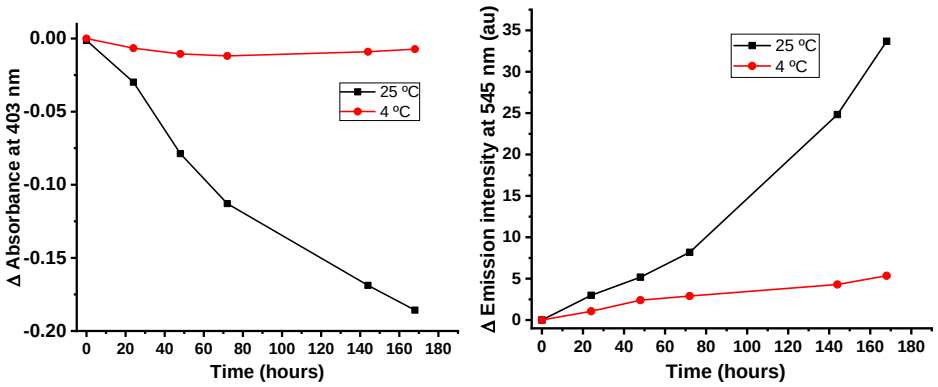

Figure 11. Evolution of the signal detected with solutions of **1** in absorbance (left) and fluorescence (right) after some hours decay of the fish samples.

The process was repeated three times and the results combined. The results showed that the variation for refrigerated samples was quite low, but the samples left at 25 °C clearly increased the emission on time. The results indicated that the changes in absorbance and fluorescence depending on time were closely related to the previous model amines. While in refrigerated samples the change in fluorescence or absorbance was not very significant, the amounts in amine concentration in the gas phase clearly increased on time for samples at 25 °C. The increase in fluorescence could be noticed by eyesight under a 366 nm light better than by the naked eye (Figure 12).

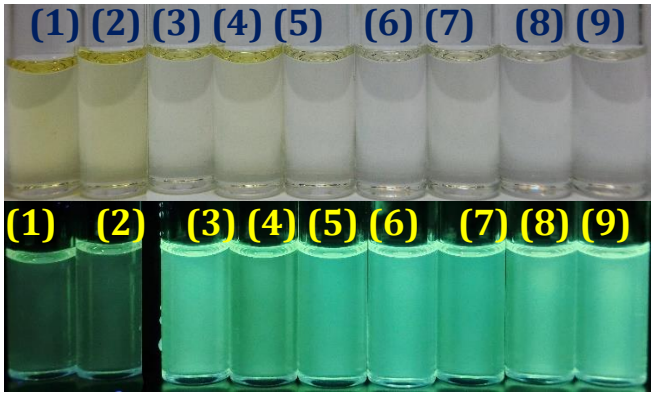

Figure 12. From left to right (1) reference **1** (1.68 × 10^{-5} M in DMSO); (2) reference+air (bubbled); (3) reference+fish sample (bubbled) (3 days at 25 °C); (4) reference+fish sample (bubbled) (1 day at 25 °C); (5) reference+histamine (bubbled); (6) reference+putrescine (bubbled); (7) reference+cadaverine (bubbled); (8) reference+pyrrolidine (bubbled); (9) reference+all amines (bubbled). (Up) under visible light. (Down) under UV light (366 nm).

Because it was easy noticed by sight inspection under a UV light, the system could be used to create an intelligent label for the detection of amines. To do so, the probe was dissolved in DMSO and a typical gelling agent (*N*-benzyloxycarbonyl-*L*-valyl-*L*-valine *n*-octadecylamide)[29] was added to the previous solution, 2 mg/0.5 ml DMSO, being 0.3% weight/volume the minimum amount possible to retain its gelation properties[30]. After that, the sample biogenic amine from rotten fish was pumped with a syringe on the probe (Figure S45 [SI]), immediately, a fading in the color and a bright fluorescence increase was noticed that lasted for a long time (Figure 13). The fluorescence decreased on time and disappeared after 12 hours.

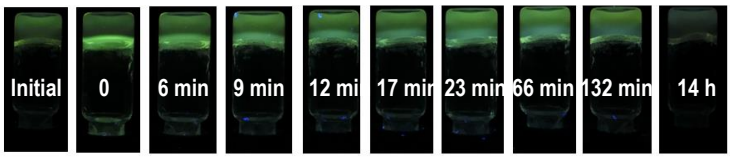

Figure 13. Response of a solution of **1**, 5·10^{-5} M in 0.25 ml of DMSO with 2 mg of gellant, after addition of amines in the gas phase, under UV light at 366 nm.

The process can be suitable for its use with suspected rotten fish without openning the packaged fish container, as a smart label for the freshness of the package (Figure 14).

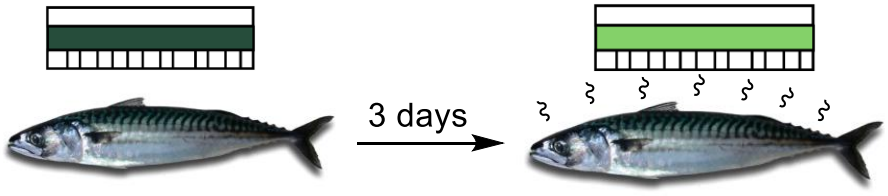

Figure 14. Fluorescence increase in presence of biogenic amines in the gas phase generated from rotten fish.

By the combined techniques developed in the process, not only fluorescence but also EPR could be used for the characterization of the freshness of fish, on the way to new examples of dual fluorescence-spin-label probes[31] or sensor arrays[32] of practical use.

3. Materials and Methods

The reactions performed with air sensitive reagents were conducted under dry nitrogen. The solvents were previously distilled under nitrogen over calcium hydride or sodium filaments. Melting points were determined in a Gallenkamp apparatus and are not corrected. Infrared spectra were registered in a Nicolet Impact 410 spectrometer in potassium bromide tablets. NMR spectra were recorded in Varian Mercury-300 and Varian Unity Inova-400 machines, in DMSO-d_6 or $CDCl_3$. Chemical shifts are reported in ppm with respect to residual solvent protons, coupling constants ($J_{X\text{-}X'}$) are reported in Hz. Mass spectra were taken in a Micromass AutoSpec machine, by electronic impact at 70 eV. Quantitative UV-visible measures were performed with a Varian Cary 300 Bio UV spectrophotometer in 1 cm UV cells thermostated at 25 °C. Fluorescence spectra were recorded in a Hitachi F-7000 FL spectrofluorometer in the range 300-700 nm, in 1 cm path length quartz cells thermostated at 25 °C. Solution X-band EPR spectra at room temperature were recorded by using flat cell on a Bruker EMX spectrometer, equipped with a Bruker ER 036TM NMR-teslameter and an Agilent 53150A microwave frequency counter to fit the magnetic field and the frequency inside the measuring cavity. Simulation of the EPR spectra was performed by using the SimFonia program and the public domain WinSim program, while spectra and graphics were plotted with Kaleidagraph v3.5 software.

Synthesis of 1-(4-methoxyphenyl-3-[4-(1-(dicyanomethyleneindan-5-yl)phenyl]-urea 1:

5-(4-Aminophenyl)indan-1-one: $Pd(PPh_3)_4$ (54 mg, 0.05 mmol) was added under nitrogen to a solution of 5-bromoindanone (410 mg, 1.94 mmol) in toluene/butanol/water 4:1:0.4 mixture (50 mL) and the mixture was stirred for 30 minutes at room temperature. Then solid 4-aminobenzeneboronic pinacol ester (447 mg, 2.04 mmol) and Na_2CO_3 (1028 mg, 9.70 mmol) were added and the mixture was heated under reflux for 16 h. Then the solvent was evaporated under reduced pressure and the residue was added to water (20 mL) and extracted with CH_2Cl_2 (5 × 40 mL). The combined organic extracts were dried (Na_2SO_4) and evaporated and the residue was purified by flash chromatography (silica, 3 × 30 cm), CH_2Cl_2, to get 5-(4-aminophenyl)indan-1-one (353 mg, 82 %) as a pale yellow solid, mp 250-251 ºC. IR (KBr, cm^{-1}): 3429, 3335, 1678 (C=O), 1592, 1297, 1278, 811. ^{1}H NMR (DMSO-d_6, 400 MHz) δ: 7.71 (s, 1H, ArH), 7.60 (s, 2H, ArH), 7.48 (d, J = 8.6 Hz, 2H, ArH), 6.68 (d, J = 8.6 Hz, 2H, ArH), 5.44 (s, br exch, 2H, NH_2), 3.10 (m, 2H, CH_2), 2.62 (m, 2H, CH_2). ^{13}C NMR & DEPT (DMSO-d_6, 400 MHz) δ: 205.44 (C=O), 156.14 (C-NH_2), 149.53, 146.91, 134.05, 127.90 (CHar), 125.84, 124.60 (CHar), 123.25 (CHar), 122.79 (CHar), 114.13 (CHar), 36.10 (CH_2), 25.44 (CH_2). MS (EI) m/z (%): 224 (M^++1, 17), 223 (M^+, 100), 195 (18), 167 (8), 152 (9), 139 (4), 117 (7), 96 (3). HRMS (EI): calcd. for $C_{15}H_{13}NO$: 223.0997 (M^+); found: 223.0998. **1-Dicyanomethylene-5-(4-aminophenyl)indane:** Malononitrile (200 mg 3.03 mmol) and DABCO (120 mg, 1.07 mmol) were added under nitrogen to 5-(4-aminophenyl)indan-1-one (200 mg, 0.90 mmol) dissolved in toluene (50 mL). The mixture was heated under reflux for 8 h and then added to water (30 mL), stirred for 5 minutes and extracted with dichloromethane (5 × 30 mL). The combined organic extracts were dried (Na_2SO_4) and the solvent evaporated under reduced pressure. The crude product was purified by flash chromatography (silica, 3 × 30 cm), from CH_2Cl_2 to CH_2Cl_2:AcOEt (15:1), to get 1-dicyanomethylene-5-(4-aminophenyl)indene (59 mg, 95 %) as an orange solid, mp: >250 ºC (decomp.), IR (KBr, cm^{-1}): 3491, 3382, 2221 (CN), 1627, 1600, 1561 (Car-Car). ^{1}H NMR (DMSO-d_6, 300 MHz) δ: 8.15 (d, J = 9.0 Hz, 1H, ArH), 7.75 (m, 2H, 2×ArH), 7.54 (d, J = 8.7 Hz, 2H, CH_2), 6.66 (d, J = 8.7 Hz, 2H, 2×ArH), 5.62 (s, br, exch, 2H, NH_2), 3.23 (m, 2H, CH_2), 3.11 (m, 2H, CH_2). ^{13}C NMR & DEPT (DMSO-d_6, 75 MHz) δ: 179.83 (C=C$(CN)_2$), 156.43, 150.35, 147.42, 132.53, 128.20 (CHar), 125.34 (CHar), 124.90 (CHar), 124.72, 121.69 (CHar), 114.36 (CN), 114.15 (CHar), 113.95 (CN), 69.86 (C$(CN)_2$), 34.65 (CH_2), 29.41 (CH_2). MS (EI) m/z (%): 272 (M^++1, 20), 271 (M^+, 100), 243 (3), 214 (2), 206 (1), 204 (2), 189 (2), 135 (2). HRMS (EI): calcd. for $C_{18}H_{13}N_3$: 271.1109 (M^+); found: 271.1108. **1-(4-methoxyphenyl-3-[4-(1-(dicyanomethyleneindan-5-yl)phenyl]urea 1:** 1-Dicyanomethylene-5-(4-aminophenyl)indane (300 mg, 1.10 mmol) was added to 4,4'-diisocyanatodiphenylether (139 mg, 0.55 mmol) dissolved in $CHCl_3$ (20 mL) and the mixture was stirred at room

temperature for 48 h. Cyclohexane (4 mL) was then added and the solid formed was filtered off, washed with $CHCl_3$ (2 × 4 mL) and dried. Compound 1-(4-methoxyphenyl-3-[4-(1-(dicyanomethyleneindan-5-yl)phenyl]urea **1** (337 mg, 77%) was obtained as a dark yellow solid, mp: >250 ºC. IR (KBr, cm^{-1}): 3316, 2221 (C≡N), 1654 (C=O), 1598, 1557, 1510, 1239, 1184, 827. ^{1}H NMR (DMSO-d_6, 400 MHz) δ: 8.90 (s, 2H, 2×NH), 8.73 (s, 2H, 2×NH), 8.25 (d, *J* = 9.0 Hz, 2H, 2×ArH), 7.91 (s, 2H, 2×ArH), 7.87 (d, *J* = 9.0 Hz, 2H, 2×ArH), 7.77 (d, *J* = 9.0 Hz, 4H, 4×ArH), 7.61 (d, *J* = 9.0 Hz, 4H, 4×ArH), 7.46 (d, *J* = 9.0 Hz, 4H, 4×ArH), 6.96 (d, *J* = 9.0 Hz, 4H, 4×ArH), 3.30 (m, 4H, 2×CH_2), 3.19 (m, 4H, 2×CH_2). ^{13}C NMR & DEPT (DMSO-d_6, 100 MHz) δ: 178.08 (C=C(CN)$_2$), 156.27, 152.46, 151.95, 146.39, 140.92, 134.93, 133.73, 131.31, 127.81 (CHar), 125.95 (CHar), 125.40 (CHar), 123.26 (CHar), 120.11 (CHar), 118.82 (CHar), 118.41 (CHar), 114.09 (CN), 113.67 (CN), 71.23 (C(CN)$_2$), 34.71 (CH_2), 29.51 (CH_2). MS (ESI) m/z (%): 795 (M^++1, 15). HRMS (ESI): calcd. for $C_{50}H_{34}N_8O_3$+H^+: 795.2827 (M^++1); found: 795.2832.

Synthesis of 1,3-bis[4-(1-dicyanomethyleneindan-5-yl)phenylureidomethyl)benzene 2:

1-Dicyanomethylene-5-(4-aminophenyl)indane (100 mg, 0.38 mmol) was added to *m*-xylylene diisocyanate (15 μL, 0.095 mmol) dissolved in $CHCl_3$ (20 mL) and the mixture was stirred at room temperature for 24 h. Then a second portion of m-xylylene diisocyanate (15 μL, 0.095 mmol) was added and the mixture was stirred for additional 24 h. The solid formed after this time was filtered off, washed with $CHCl_3$ (2 × 2 mL) and dried under reduced pressure. Compound 1,3-bis[4-(1-dicyanomethyleneindan-5-yl)phenylureidomethyl)benzene **2** (104 mg, 75%) was obtained as a yellow solid, mp: 212-214 ºC. IR (KBr, cm^{-1}): 3328, 2221 (C≡N), 1658 (C=O), 1604, 1557, 1320, 1219, 1184. ^{1}H NMR (DMSO-d_6, 400 MHz) δ: 8.82 (s, 2H, NH), 8.17 (d, *J* = 9.0 Hz, 2H, 2×ArH), 7.82 (s, 2H, 2×ArH), 7.79 (d, *J* = 9.0 Hz, 2H, 2×ArH), 7.65 (d, *J* = 8.6 Hz, 4H, 4×ArH), 7.52 (d, *J* = 8.6 Hz, 4H, 4×ArH), 7.29 (m, 2H, 2×ArH), 7.20 (m, 2H, 2×ArH), 6.71 (t, *J* = 6.0 Hz, 2H, 2×NH), 4.32 (d, *J* = 6.0 Hz, 4H, 2×CH_2), 3.28 (m, 2H, CH_2), 3.15 (m, 2H, CH_2). ^{13}C NMR & DEPT ($CDCl_3$, 100 MHz) δ: 179.60 (C=C(CN)$_2$), 155.78, 154.63, 146.04, 141.21, 140.00, 133.07, 130.10, 128.22 (CHar), 127.58 (CHar), 125.72, 125.67 (CHar), 125.55 (CHar), 125.22 (CHar), 122.60 (CHar), 117.54 (CHar), 113.66 (CN), 113.25 (CN), 70.61 (C(CN)$_2$), 42.32 (2×CH_2), 34.24 (CH_2), 29.04 (CH_2). MS (ESI) m/z (%): 753.27 (M^++Na^+, 94), 731.29 (M^++1, 100). HRMS (ESI): calcd. for $C_{46}H_{34}N_8O_2$+H^+: 731.2877 (M^++1); found: 731.2864.

Synthesis of 1-(4-methoxyphenyl-3-[4-(1-(dicyanomethyleneindan-5-yl)phenyl]-urea 3:

1-Dicyanomethylene-5-(4-aminophenyl)indane (150 mg, 0.55 mmol) was added to *p*-methoxyphenyl isocyanate (82 mg, 0.55 mmol) dissolved in $CHCl_3$ (10 mL) and the mixture was stirred at room temperature for 48 h. Cyclohexane (3 mL) was then added and the solid formed was filtered off, washed with $CHCl_3$ (2 × 2 mL) and dried. Compound 1-(4-methoxyphenyl-3-[4-(1-(dicyanomethyleneindan-5-yl)phenyl]urea **3** (172 mg, 74%) was obtained as a dark yellow solid, mp: 232-233 ºC. IR (KBr, cm^{-1}): 3320, 2221 (CN), 1658 (C=O), 1596, 1557, 1510, 1239, 1184, 1029, 823. ^{1}H NMR (DMSO-d_6, 300 MHz) δ: 8.85 (s, 1H, NH), 8.56 (s, 1H, NH), 8.23 (d, *J* = 9.0 Hz, 1H, ArH), 7.90 (s, 1H, ArH), 7.86 (d, *J* = 9.0 Hz, 1H, ArH), 7.76 (d, *J* = 9.0 Hz, 2H, ArH), 7.58 (d, J = 9.0 Hz, 2H, ArH), 7.37 (d, J = 9.0 Hz, 2H, ArH), 6.87 (d, *J* = 9.0 Hz, 2H, ArH), 3.82 (s, 3H, CH_3), 3.28 (m, 2H, CH_2), 3.18 (m, 2H, CH_2). ^{13}C NMR & DEPT (DMSO-d_6, 75 MHz) δ: 180.04 (C=C(CN)$_2$), 156.22, 154.52, 152.47, 146.33, 141.02, 133.63, 132.44, 131.05, 127.74 (CHar), 125.86 (CHar), 125.34 (CHar), 123.15 (CHar), 120.07 (CHar), 118.23 (CHar), 114.06 (CN), 113.94 (CHar), 113.63 (CN), 71.12 (C(CN)$_2$), 55.13 (OCH_3), 34.63(CH_2), 29.45 (CH_2). MS (EI) m/z (%): 421 (M^++1, 3), 420 (M^+, 11), 297 (100), 271 (87), 149 (17), 123 (31). HRMS (EI): calcd. for $C_{26}H_{20}N_4O_2$: 420.1586 (M+); found: 420.1582.

Synthesis of 1-[4-(*N,N*-dimethylamino)phenyl]-3-[4-(1-(dicyanomethyleneindan-5-yl)phenyl]urea 4:

1-Dicyanomethylene-5-(4-aminophenyl)indane (150 mg, 0.55 mmol) was added to *p*-*N,N*-dimethylaminophenyl isocyanate (89 mg, 0.55 mmol) dissolved in $CHCl_3$ (10 mL) and

the mixture was stirred at room temperature for 48 h. Cyclohexane (3 mL) was then added and the solid formed was filtered off, washed with $CHCl_3$ (2 × 2 mL) and dried. Compound 1-[4-(*N,N*-dimethylamino)phenyl]-3-[4-(1-(dicyanomethylene-indan-5-yl)phenyl]urea **4** (160 mg, 67%) was obtained as a dark yellow solid, mp: 178-179 ºC. IR (KBr, cm^{-1}): 3320, 2221 (C≡N), 1654 (C=O), 1596, 1565, 1518, 1320, 1242, 1185, 823. ^{1}H NMR (DMSO-d_6, 300 MHz) δ: 8.81 (s, 1H, NH), 8.41 (s, 1H, NH), 8.25 (d, *J* = 9.0 Hz, 1H, ArH), 7.92 (s, 1H, ArH), 7.88 (d, *J* = 9.0 Hz, 1H, ArH), 7.76 (d, *J* = 9.0 Hz, 2H, 2×ArH), 7.60 (d, *J* = 9.0 Hz, 2H, 2×ArH), 7.29 (d, *J* = 9.0 Hz, 2H, 2×ArH), 6.72 (d, *J* = 9.0 Hz, 2H, 2×ArH), 3.30 (m, 2H, CH_2), 3.20 (m, 2H, CH_2), 2.84 (s, 6H, 2×CH_3). ^{13}C NMR & DEPT (DMSO-d_6, 75 MHz) δ: 180.06 (C=C(CN)2), 156.49, 152.63, 146.60, 141.28, 133.67, 130.96, 129.26, 127.80 (CHar), 125.89 (CHar), 125.42 (CHar), 123.16 (CHar), 120.32 (CHar), 118.22 (CHar), 117.54, 114.15 (CN), 113.73 (CN), 113.16 (CHar), 71.07 ($C(CN)_2$), 40.64 ($N(CH_3)_2$), 34.61 (CH_2), 29.43 (CH_2). MS (EI) m/z (%): 433 (M^+, 5), 297 (100), 271 (92), 162 (35), 136 (37). HRMS (EI): calcd. for $C_{27}H_{23}N_5O$: 433.1903 (M^+); found: 433.1907.

Synthesis of 1-(4-methylthiophenyl)-3-[4-(1-(dicyanomethyleneindan-5-yl)phenyl]urea 5:

1-Dicyanomethylene-5-(4-aminophenyl)indane (150 mg, 0.55 mmol) was added to *p*-methylthiophenyl isocyanate (91 mg, 0.55 mmol) dissolved in $CHCl_3$ (10 mL) and the mixture was stirred at room temperature for 48 h. Cyclohexane (3 mL) was then added and the solid formed was filtered off, washed with $CHCl_3$ (2 × 2 mL) and dried. Compound 1-(4-methylthiophenyl)-3-[4-(1-(dicyanomethyleneindan-5-yl)-phenyl]urea **5** (173 mg, 72%) was obtained as a dark yellow solid, mp: 209-210 ºC. IR (KBr, cm^{-1}): 3317, 2221 (CN), 1654 (C=O), 1596, 1546, 1495, 1324, 1281, 1192, 827. ^{1}H NMR (DMSO-d_6, 400 MHz) δ: 8.91 (s,1H, NH), 8.77 (s,1H, NH), 8.25 (d, *J* = 9.0 Hz, 1H, ArH), 7.91 (s, 1H, ArH), 7.87 (d, *J* = 9.0 Hz, 1H, ArH), 7.77 (d, *J* = 9.0 Hz, 2H, ArH), 7.60 (d, *J* = 9.0 Hz, 2H, ArH), 7.44 (d, *J* = 9.0 Hz, 2H, ArH), 7.23 (d, *J* = 9.0 Hz, 2H, ArH), 3.30 (m, 2H, CH2), 3.19 (m, 2H, CH_2), 2.44 (s, 3H, CH_3). ^{13}C NMR & DEPT (DMSO-d_6, 75 MHz) δ: 180.05 ($C=C(CN)_2$), 156.23, 152.28, 146.35, 140.80, 137.20, 133.72, 131.36, 130.17, 127.78 (CHar), 127.70 (CHar), 125.94 (CHar), 125.38 (CHar), 123.25 (CHar), 119.06 (CHar), 118.42 (CHar), 114.06 (CN), 113.64 (CN), 71.23 ($C(CN)_2$), 34.69 (CH_2), 29.50 (CH_2), 15.94 (CH_3). MS (EI) m/z (%): 436 (M^+, 7), 297 (100), 271 (93), 165 (32). HRMS (EI): calcd. for $C_{26}H_{20}N_4OS$: 436.1358 (M^+); found: 436.1359.

Synthesis of *N,N*-bis-[4-(1-(dicyanomethyleneindan-5-yl)phenyl]pyridine-2,6-dicarboxamide 6:

2,6-Pyridinedicarbonyl dichloride (75 mg, 0.37 mmol) dissolved in dichloromethane (10 mL) was added dropwise to a chilled and stirred solution of 1-dicyanomethylene-5-(4-aminophenyl)indane (200 mg, 0.74 mmol) and *N,N*-diisopropylethylamine (96 mg, 0.74 mmol) in dichloromethane (50 mL). The mixture was left to warm to room temperature and stirred for 24 hours. The solid formed was filtered off, washed with $CHCl_3$ (2 × 3 mL) and dried. Compound *N,N*-bis-[4-(1-(dicyanomethyleneindan-5-yl)phenyl]pyridine-2,6-dicarboxamide **6** (197 mg, 79%) was obtained as a dark yellow solid, mp: >250 ºC. IR (KBr, cm^{-1}): 3344, 2221 (C≡N), 1682 (C=O), 1565, 1526, 1340, 1188, 819. 1H NMR ($CDCl_3$, 400 MHz) δ (ppm): 10.79 (s, 2H, 2×NH), 8.51 (d, *J* = 12.0 Hz, 2H, 2×ArH), 8.42 (d, *J* = 12.0 Hz, 2H, 2×ArH), 8.16 (d, *J* = 12.0 Hz, 2H, 2×ArH), 8.10 (d, *J* = 9.0 Hz, 4H, 4×ArH), 7.72 (m, 8H, 8×ArH), 3.30 (m, 4H, 2×CH_2), 3.24 (m, 4H, 2×CH_2). ^{13}C NMR & DEPT (DMSO-d_6, 75 MHz) δ: 179.95 ($C=C(CN)_2$), 161.74, 156.13, 148.69, 146.00, 139.99 (CHar), 139.00, 134.04, 133.80, 127.65 (CHar), 127.05, 126.20 (CHar), 125.35 (CHar), 123.61 (CHar), 121.09 (CHar), 113.93 (CN), 113.52 (CN), 71.50 ($C(CN)_2$), 34.65 (CH_2), 29.48 (CH_2). MS (ESI) m/z (%): 674 (M^++1, 12). HRMS (EI): calcd. for $C_{43}H_{27}N_7O_2$+H^+: 674.2299 (M^+); found: 674.2295.

Synthesis of 5,5'-(((6-cyclohexyl-[3,4'-bipyridine]-2',6'-dicarbonyl)bis(piperazine-4,1-diyl))bis(pyridine-6,3-diyl))bis(indan-1-one) 7:

6-(Piperidin-1-yl)-[3,4'-bipyridine]-2',6'-dicarboxylic acid: $Pd(PPh_3)_4$ (58 mg, 0.05 mmol) was added under nitrogen to a solution of dimethyl 4-bromopyridine-2,6-dicarboxylate (822 mg, 3.0 mmol) in tetrahydrofuran (120 mL) and the mixture was stirred for 30 minutes at room temperature. Then solid 2-(piperidin-1-yl)-5-(4,4,5,5-tetramethyl-1,3,2-

dioxaborolan-2-yl)pyridine (865 mg, 3.0 mmol) and cesium carbonate (1.47 g, 4.5 mmol) dissolved in water (15 mL) were successively added and the mixture was heated under reflux for 24 h. Then the solvent was evaporated under reduced pressure and the residue was suspended in water (10 mL). Then NaOH solution (5% w/v in H_2O) was added dropwise until pH = 10 and the mixture was dissolved in tetrahydrofuran (60 mL) and heated under reflux for 1 hour until complete hydrolysis of diester and monoester mixture. Then the mixture was chilled within an ice bath and HCl solution (35% w/v in water) was added drowise until pH = 1. Then the solvent was evaporated until reduced pressure and the solid residue was dried under vacuum. The solid residue was suspended in anhydrous dichloromethane (125 mL) under nitrogen and then oxalyl chloride (3.00 g, 24 mmol) and anhydrous dimethylformamide (0.2 mL) were added and the mixture was stirred overnight. Then the solvent and the excess of oxalyl chloride were evaporated under reduced pressure and anhydrous methanol (5 mL, 124 mmol) in dichloromethane (60 mL) was added under nitrogen and the mixture was stirred overnight. Then the solvent was evaporated under reduced pressure and the residue was purified by flash chromatography (silica, 3 x 50 cm), from CH_2Cl_2 to CH_2Cl_2/MeOH 9:1 v/v to get dimethyl 6-(piperidin-1-yl)[3,4'-bipyridine]-2',6'-dicarboxylate as a light yellow solid (522 mg, 49 %), mp: 146–148 ºC, Rf (DCM/MeOH, 50:3): 0.83; ^{1}H RMN ($CDCl_3$, 300 MHz): δ = 8.63 (s, 1H, ArH); 8.47 (s, 2H, ArH); 7.87-7.83 (dd, *J* = 9.3 Hz, 1H, ArH); 6.75-6.72 (d, *J* =9.3 Hz, 1H, ArH); 4.04 (m, 6H, 3xCH_2); 3.66 (m, 4H, 3xCH_2); 1.68 (m, 9H, 3xCH_2); ^{13}C RMN ($CDCl_3$, 75 MHz): δ = 165.4 (C=O), 159.6 (C_{Ar}), 148.7 (CH_{Ar}), 148.6 (CH_{Ar}), 147 (CH_{Ar}), 135.5 (C_{Ar}), 123.6 (CH_{Ar}), 119.1 (C_{Ar}), 106.5 (CH_{Ar}), 53.4 (CH_3), 45.9 (CH_2), 25.5 (CH_2), 24.7 (CH_2); MS (EI) m/z (%): 355 (M^+, 100), 326 (55), 312 (30), 299 (20), 272 (32), 84 (28); HRMS (EI): calcd. for $C_{19}H_{21}N_3O_4$: 355.1532; found 355.1535. Diester (512 mg, 1.44 mmol) was dissolved in a mixture of tetrahydrofuran (10 mL) and water (1 mL) and a solution of NaOH (5% w/v in H_2O) was added dropwise until pH = 10 and the mixture was heated under reflux for 1 hour until complete hydrolysis of diester. Then the mixture was chilled within an ice bath and HCl solution (35% w/v in water) was added dropwise until pH = 1. Then the solvent was evaporated until reduced pressure and the solid residue was extracted several times with dichloromethane/methanol 1:1 until complete extraction of diacid. Evaporation of solvent under reduced pressure afforded pure 6-(piperidin-1-yl)-[3,4'-bipyridine]-2',6'-dicarboxylic acid as a light yellow solid (448 mg, 95 % from diester, 47% from dimethyl 4-bromopyridine-2,6-dicarboxylate), mp: 244-246 ºC (decomp.); ^{1}H RMN (CD_3OD, 300MHz): δ = 8.49 (s, 2H, ArH); 8.43 (s, 0.3H, ArH); 8.28 (s, 0.7H, ArH); 8.14-8.11 (d, *J* = 9.3 Hz, 1H, ArH); 7.10-7.07 (d, *J* =9.3 Hz, 1H, ArH); 3.66 (m, 4H, 3xCH_2); 1.69 (m, 6H, 3xCH_2); ^{13}C RMN (CD_3OD, 75 MHz): δ = 167.4 and 166.4 (C=O), 150.8 (C_{Ar}), 149.9 (CH_{Ar}), 140.2 (CH_{Ar}), 131.2 (CH_{Ar}), 128.8 (C_{Ar}), 124.7 (CH_{Ar}), 121.1 (C_{Ar}), 111.4 (CH_{Ar}), 26.6 (CH_2), 25.2 (CH_2); IR (KBr): 3609 (OH), 2786, 2167, 1648, 1340, 1108, 752 cm^{-1}; MS (EI) m/z (%): 327 (M^+, 75), 283 (92), 239 (45), 157 (41), 84 (100). HRMS (EI): calcd. for $C_{17}H_{17}N_3O_4$+H^+: 328.1292; found: 328.1291.

5,5'-(((6-Cyclohexyl[3,4'-bipyridine]-2',6'-dicarbonyl)bis(piperazine-4,1-diyl))bis(pyridine-6,3-diyl))bis(indan-1-one) 7: Oxalyl chloride (530.0 μL, ϱ= 1.478 g/mL, 6.17 mmol) was added to a suspension of 6-cyclohexyl-[3,4'-bipyridine]-2',6'-dicarboxylic acid (294 mg, 0.90 mmol) in CH_2Cl_2 (100 mL) with 3 drops of DMF as catalyst. The mixture was stirred at room temperature for 24 hours and then the solvent and the excess of oxalyl chloride were evaporated under reduced pressure. A solution of 1-dicyanomethylene-5-(4-aminophenyl)indane (190 mg, 0.70 mmol) in DMF (55 mL) was added over the white solid in an ice bath. Then, *N*,*N*-diisopropylethylamine (200 μL, ϱ= 0.742 g/mL, 1.15 mmol) and a spatula tip of 4-dimethylaminopyridine (DMAP) were added and the mixture was stirred at 0 ºC for 15 minutes and then at room temperature for 24 hours. A yellow precipitate formed that was filtered off. The filtered solid was washed up with $CHCl_3$ (3 × 10 mL) and CH_2Cl_2 (3 × 5 mL). Finally, the solid was collected and the traces of solvent evaporated under reduced pressure to get 5,5'-(((6-cyclohexyl-[3,4'-bipyridine]-2',6'-dicarbonyl)bis(piperazine-4,1-diyl))bis(pyridine-6,3-diyl))bis(indan-1-one) **7** (466 mg, 62%) as an orange solid, almost insoluble in all common solvents, mp: 212-213 ºC (decomp.); IR

(KBr, cm^{-1}): 3626 (NH), 3069, 2360, 2218, 1648 (C=O), 1558, 1527, 1337, 1188, 1122, 1005 cm^{-1}; ^1H NMR (DMSO-d_6, 400 MHz) δ: 11.21 (s, 2H, 2xNH), 8.72 (s, 1H, ArH), 8.61 (s, 2H, ArH), 8.31 (d, *J* = 8.4 Hz, 2H, ArH), 8.21 (m, 2H, ArH), 8.17 (d, *J* = 8.4 Hz, 4H, ArH), 8.00 (s, 2H, ArH), 7.95 (d, *J* = 8.8 Hz, 7H, ArH), 7.08 (d, *J* = 7.2 Hz, 1H, ArH), 3.70 (m, 4H, 2xCH_2)), 3.35 (m, 4H, 2xCH_2), 3.24 (m, 4H, 2xCH_2), 1.68 (m, 2H, CH_2), 1.61 (m, 4H, 2xCH_2); MS (FAB) m/z (%): 833 (M^+, 2), 834 (4), 835 (10), 836 (6), 837 (3). HRMS (EI): calcd. for $C_{53}H_{39}N_9O_2$+H^+: 834.3299; found: 834.3298.

5. Conclusions

In conclusion, we have described a rare class of persistent radicals formed by interaction of fluorogenic arylurea derivatives and primary or secondary amines in the presence of light, water and air. The most persistent term of the series was studied by spectroscopic techniques as well as quantum mechanics calculations. All results pointed to a rare case of photoinduced proton-coupled electron transfer, although the slow kinetics of formation and the evolution of the radical species from a formerly fluorescent transient intermediate rendered the system more complicate than classic examples. The two best examples of formation of radicals having a well resolved EPR hyperfine structure and high intensity came from a well-known selective fluorogenic probe for biogenic amines or a fluorescent probe for ω-aminoacids, therefore adding a new perspective to these and other to-be-performed fluorescent probes. These chemical probes are the first examples of multi-signal reporters for the discrimination between primary, secondary and tertiary amines in which the usual signaling report by UV-visible or fluorescent signal is complemented by paramagnetic signaling of the same samples at different reporting times. The selectivity of the chemical probes for different types of amines and the large types of signaling offered by these probes, from now including paramagnetic species, made them good starting points for the preparation of multi-signaling chemical probes for the detection of important organic metabolites. As an immediate application, we have developed a multi-signal smart label for the quick inspection of freshness in fish.

Supplementary Materials: The following are available online at www.mdpi.com/xxx/s1: complete characterization of all compounds, additional EPR measurements, UV-Vis titrations, fluorescence measurements, detection of biogenic amines and quantum chemical calculations.

Author Contributions: "Conceptualization, T.T.; methodology, EPR spectroscopy, J.G.-T.; investigation, UV-vis and fluorescence spectroscopy, B.D.G.; investigation, synthesis, B.D.G., C.H.-M., M.M.S.; investigation, food technology, M.J.R.; data curation, J.G.-C.; quantum chemical calculations, J.V.C.; writing—original draft preparation, B.D.G., J.G.-C., T.T.; writing—review and editing, T.T.; "All authors have read and agreed to the published version of the manuscript."

Funding: "This research was funded by the NATO Science for Peace and Security Programme (Grant SPS G5536), the Junta de Castilla y León, Consejería de Educación y Cultura y Fondo Social Europeo (Grant BU263P18) and the Ministerio de Ciencia e Innovación (Grant PID2019-111215RB-100)."

Conflicts of Interest: "The authors declare no conflict of interest."

Sample Availability: Samples of the compounds **1**-**7** are available from the authors.

References

1. Casu, M. B. Nanoscale Studies of Organic Radicals: Surface, Interface, and Spinterface. *Acc. Chem. Res.* **2018**, *51*, 753–760. doi.org/10.1021/acs.accounts.7b00612
2. Miller, J.S. Organic- and molecule-based magnets. *Mater. Today*, **2014**, *17*, 224-235. doi.org/10.1016/j.mattod.2014.04.023
3. Saito, G.; Yoshida, Y. Frontiers of organic conductors and superconductors. *Top. Curr. Chem.* **2012**, *312*, 67-126. DOI: 10.1007/128_2011_224
4. Gobbi, M.; Novak, M.A.; Del Barco, E. Molecular spintronics. *J. Appl. Phys.* **2019**, *125*, 240401. doi.org/10.1063/1.5113900

5. Mas-Torrent, M.; Rovira, C.; Veciana, J. Surface-Confined Electroactive Molecules for Multistate Charge Storage Information. *Adv. Mater*. **2013**, *25*, 462-468. doi.org/10.1002/adma.201201510
6. Ravelli, D.; Fagnoni, M.; Albini, A. Photoorganocatalysis. What for?. *Chem. Soc. Rev.* **2013**, *42*, 97-113. doi.org/10.1039/C2CS35250H
7. Zheng, R.; Shi, Y.; Jia, Z.; Zhao, C.; Zhang, Q.; Tan, X. Fast repair of DNA radicals. *Chem. Soc. Rev.* **2010**, *39*, 2827-2834. 10.1039/B924875G
8. Naoki Shida1, Yasushi Imada1, Shingo Nagahara1, Yohei Okada2 & Kazuhiro Chiba1 Interplay of arene radical cations with anions and fluorinated alcohols in hole catalysis. *Commun. Chem.* **2019**, *2*, 24. doi.org/10.1038/s42004-019-0125-4
9. Lü, B.; Chen, Y.; Li, P.; Wang, B.; Müllen, K.; Yin, M. Stable radical anions generated from a porous perylenediimide metal-organic framework for boosting near-infrared photothermal conversion. *Nat. Commun.* **2019**, *10*, 767. doi.org/10.1038/s41467-019-08434-4
10. Hankache, J.; Wenger, O.S. Organic Mixed Valence. *Chem. Rev.* **2011**, *111*, 5138-5178. doi.org/10.1021/cr100441k
11. Fekete, A.; Malik, A.K.; Kumar, A.; Schmitt-Kopplin, P. Amines in the Environment *Crit. Rev. Anal. Chem.* **2010**, *40*, 102-121. doi.org/10.1080/10408340903517495
12. Pradhan, T.; Jung, H.S.; Jang, J.H.; Kim, T.W.; Kang, C.; Kim, J.S. Chemical sensing of neurotransmitters. *Chem. Soc. Rev.* **2014**, *43*, 4684-4713. doi.org/10.1039/C3CS60477B
13. Doeun, D.; Davaatseren, M.; Chung, M.-S. Biogenic amines in foods. *Food Sci. Biotechnol.* **2017**, *26*, 1463–1474. doi.org/10.1007/s10068-017-0239-3
14. Kumpf, J.; Freudenberg, J.; Fletcher, K.; Dreuw, A.; Bunz, U. H. F. Detection of Amines with Extended Distyrylbenzenes by Strip Assays. *J. Org. Chem.* **2014**, *79*, 6634-6645. doi.org/10.1021/jo501129d
15. Zhou, Y.; Gao, H.; Zhu, F.; Ge, M.; Liang, G. Sensitive and rapid detection of aliphatic amines in water using self-stabilized micelles of fluorescent block copolymers. *J. Hazard. Mater.* **2019**, *368*, 630-637. doi.org/10.1016/j.jhazmat.2019.01.097
16. Rochat, S.; Swager, T. M. Fluorescence sensing of amine vapors using a cationic conjugated polymer combined with various anions. *Angew. Chem. Int. Ed.* **2014**, *53*, 9792-9796. doi.org/10.1002/anie.201404439
17. H. Iida, M. Miki, S. Iwahana, E. Yashima, Riboflavin-Based Fluorogenic Sensor for Chemo- and Enantioselective Detection of Amine Vapors *Chem. Eur. J.* **2014**, *20*, 4257-4262. 10.1002/chem.201400234
18. Yang, X.; Zhou, J.; Li, Y.; Yan, M.; Cui, Y.; Sun, G. A reaction-based sensing scheme for volatile organic amine reagents with the chromophoric-fluorogenic dual mode. *Spectrochim. Acta A Mol. Biomol. Spectrosc.* **2020**, *240*, 118539. doi.org/10.1016/j.saa.2020.118539
19. Moreno, D.; Díaz de Greñu, B.; García, B.; Ibeas, S.; Torroba, T. A turn-on fluorogenic probe for detection of MDMA from ecstasy tablets *Chem. Commun.* **2012**, *48*, 2994-2996. doi.org/10.1039/C2CC17823K
20. Moreno, D.; Cuevas, J.V.; García-Herbosa, G.; Torroba, T. A fluorescent molecular ruler as a selective probe for ω-aminoacids. *Chem. Commun.* **2011**, *47*, 3183-3185. doi.org/10.1039/C0CC05454B
21. Barrio-Manso, J.L.; Calvo, P.; García, F.C.; Pablos, J.L.; Torroba, T.; García, J.M. Functional fluorescent aramids: aromatic poly-amides containing a dipicolinic acid derivative as luminescent converters and sensory materials for the fluorescence detection and quantification of Cr(VI), Fe(III) and Cu(II). *Polym. Chem.*, **2013**, *4*, 4256-4264. doi.org/10.1039/C3PY00503H
22. Aragay, G.; Frontera, A.; Lloveras, V.; Vidal-Gancedo, J.; Ballester, P. Different Nature of the Interactions between Anions and HAT(CN)6: From Reversible Anion−π Complexes to Irreversible Electron-Transfer Processes (HAT(CN)6 = 1,4,5,8,9,12-Hex-aazatriphenylene). *J. Am. Chem. Soc.* **2013**, *135*, 2620-2627. doi.org/10.1021/ja309960m
23. Yadav, S.; Ghosh, S.; Ajayakumar, M.R.; Mukhopadhyay, P. Single-Electron Transfer Driven Cyanide Sensing: A New Multi-modal Approach. *Org. Lett.* **2010**, *12*, 2646-2649. doi.org/10.1021/ol1008558
24. A. D. Becke, Density-functional thermochemistry. III. The role of exact exchange. *J. Chem. Phys.* **1993**, *98*, 5648-5652. doi.org/10.1063/1.464913
25. C. T. Lee, W. T. Yang, R. G. Parr, Development of the Colle-Salvetti correlation-energy formula into a functional of the electron density *Phys. Rev. B* **1988**, *37*, 785-789. doi.org/10.1103/PhysRevB.37.785
26. M. J. Frisch, G. W. Trucks, H. B. Schlegel, G. E. Scuseria, M. A. Robb, J. R. Cheeseman, J. A. Montgomery, Jr., T. Vreven, K. N. Kudin, J. C. Burant, J. M. Millam, S. S. Iyengar, J. Tomasi, V. Barone, B. Mennucci, M. Cossi, G. Scalmani, N. Rega, G. A. Petersson, H. Nakatsuji, M. Hada, M. Ehara, K. Toyota, R. Fukuda, J. Hasegawa, M. Ishida, T. Nakajima, Y. Honda, O. Kitao, H. Nakai, M. Klene, X. Li, J. E. Knox, H. P. Hratchian, J. B. Cross, C. Adamo, J. Jaramillo, R. Gomperts, R. E. Stratmann, O. Yazyev, A. J. Austin, R. Cammi, C. Pomelli, J. W. Ochterski, P. Y. Ayala, K. Morokuma, G. A. Voth, P. Salvador, J. J. Dannenberg, V. G. Zakrzewski, S. Dapprich, A. D. Daniels, M. C. Strain, O. Farkas, D. K. Malick, A. D. Rabuck, K. Raghavachari, J. B. Foresman, J. V. Ortiz, Q. Cui, A. G. Baboul, S. Clifford, J. Cioslowski, B. B. Stefanov, G. Liu, A. Liashenko, P. Piskorz, I. Komaromi, R. L. Martin, D. J. Fox, T. Keith, M. A. Al-Laham, C. Y. Peng, A. Nanayakkara, M. Challacombe, P. M. W. Gill, B. Johnson, W. Chen, M. W. Wong, C. Gonzalez and J. A. Pople, *Gaussian 03, Revision C.02*, Gaussian, Inc., Wallingford, CT, 2004.
27. Kepler, S.; Zeller, M.; Rosokha, S.V. Anion−π Complexes of Halides with p-Benzoquinones: Structures, Thermodynamics, and Criteria of Charge Transfer to Electron Transfer Transition. *J. Am. Chem. Soc.* **2019**, *141*, 9338–9348. doi.org/10.1021/jacs.9b03277
28. Migliore, A.; Polizzi, N.F.; Therien, M.J.; Beratan, D.N. Biochemistry and Theory of Proton-Coupled Electron Transfer. *Chem. Rev.* **2014**, *114*, 3381-3465. doi.org/10.1021/cr4006654
29. Hanabusa, K.; Tange, J.; Taguchi, Y.; Koyama, T.; Shirai, H. Small Molecular Gelling Agents to Harden Organic Liquids: Alkyl-amide of N-Benzyloxycarbonyl-L-valyl-L-valine. *J. Chem. Soc., Chem. Commun*., **1993**, 390-392. doi.org/10.1039/C39930000390

30. Hanabusa, K.; Suzuki, M. Development of low-molecular-weight gelators and polymer-based gelators. *Polym. J.* **2014**, *46*, 776–782. doi.org/10.1038/pj.2014.64
31. Dong, P.; Stellmacher, J.; Bouchet, L.M.; Nieke, M.; Kumar, A.; Osorio-Blanco, E.R.; Nagel, G.; Lohan, S.B.; Teutloff, C.; Patzelt, A.; Schäfer-Korting, M.; Calderón, M.; Meinke, M.C.; Alexiev, U. A Dual Fluorescence-Spin Label Probe for Visualization and Quantification of Target Molecules in Tissue by Multiplexed FLIM – EPR Spectroscopy. *Angew. Chem. Int. Ed.* **2021**, just accepted doi.org/10.1002/anie.202012852
32. Hu, Y.; Zhou, Z.; Zhao, F.; Liu, X.; Gong, Y.; Xiong, W.; Sillanpää, M. Fingerprint Detection and Differentiation of Gas-phase Amines Using a Fluorescent Sensor Array Assembled from Asymmetric Perylene Diimides. *Sci. Rep.* **2018**, *8*, 10277. 10.1038/s41598-018-28556-x